

## Active steering of laser-accelerated ion beams

O. Lundh,<sup>a)</sup> Y. Glinec, C. Homann, F. Lindau, A. Persson, and C.-G. Wahlström  
*Department of Physics, Lund University, P.O. Box 118, S-22100 Lund, Sweden*

D. C. Carroll and P. McKenna  
*SUPA, Department of Physics, University of Strathclyde, Glasgow G4 0NG, United Kingdom*

(Received 15 September 2007; accepted 17 December 2007; published online 10 January 2008)

A technique for optical control of the spatial distribution of laser-accelerated ion beams is presented. An ultrashort laser pulse, tightly focused to relativistic intensities on a thin foil target, drives a beam of MeV ions. An auxiliary, nanosecond laser pulse drives a shock and locally deforms the initially flat target prior to the main pulse interaction. By changing the properties of the shock-driving laser pulse, the normal direction of the ion emitting surface is locally manipulated and the emission direction is thereby controlled. In the future, this method could be used to achieve dynamic control of the ion beam divergence. © 2008 American Institute of Physics. [DOI: 10.1063/1.2832765]

Proton and heavy ion acceleration, driven by ultraintense laser-plasma interactions in thin foil targets is currently drawing significant scientific interest. The generated beams have several attractive characteristics, such as high laser-to-particle energy conversion efficiency,<sup>1</sup> very low emittance,<sup>2</sup> and a small virtual source size.<sup>3</sup> Proposed applications of this potentially compact ion beam source include ion radiotherapy for cancer treatment,<sup>4</sup> isotope production for medical imaging techniques,<sup>5</sup> injectors for large accelerators,<sup>6</sup> and ignitors in laser-driven inertial confinement fusion.<sup>7</sup>

Many different mechanisms can lead to the generation of fast ion beams.<sup>8</sup> At an intensity of the order of  $10^{19}$  W/cm<sup>2</sup>, rear surface sheath acceleration dominates and generates the most energetic particles.<sup>9</sup> Electrons, heated to MeV temperatures by the intense laser field at the front, traverse the thin foil target and establish exceptionally high ( $\sim$ TV/m) electrostatic fields at the rear surface. Hydrogen atoms, present on the target surface under typical experimental vacuum conditions, are rapidly field ionized and the protons accelerated. The direction of the accelerating field is defined by the target geometry and, for a plane target foil, the emitted proton beam is centered on the target normal axis, regardless of the laser incidence angle. By shaping the rear surface, it is possible to control the proton emission. In particular, numerical simulations and experiments have shown that a prefabricated concave or convex rear surface produce converging or diverging proton beams, respectively.<sup>9–11</sup> It has also been shown that the target foil can be significantly deformed by a shock wave, launched by amplified spontaneous emission (ASE) prior to the main pulse arrival, and that this dynamic deformation can, under oblique laser irradiation, significantly shift the proton beam emission direction.<sup>12,13</sup> The first method for controlling the proton beam divergence requires prefabricated curved targets, a potential drawback for future applications requiring ultrathin targets<sup>14</sup> and high repetition rates. The second method facilitates dynamic control of the emission direction using standard flat foils, but is limited since the position and the spatial intensity distribution of the ASE are difficult to control independently of the main pulse. In the present experiment, schematically illustrated in Fig. 1, a separate nanosecond laser pulse is used to drive a shock

and locally shape the target foil prior to the main pulse interaction. By careful selection of the intensity, arrival time and position of this steering pulse relative to the main pulse, we control the local slope of the target rear surface and gain active control of the proton emission direction.

The experiment is performed using the 10 Hz multiterawatt laser at the Lund Laser Centre in Sweden. It is a Ti:sapphire system, based on the chirped pulse amplification scheme and operating at 800 nm, delivering for this experiment 600 mJ of laser energy on the target in a 45 fs [full width at half maximum (FWHM)] pulse. The laser beam is focused using an  $f/3$  off-axis parabolic mirror to a 5  $\mu$ m (FWHM) spot, yielding an inferred peak intensity exceeding  $4 \times 10^{19}$  W/cm<sup>2</sup>. In focus, 3  $\mu$ m thick aluminum foils are positioned for  $p$ -polarized irradiation at 30° angle of incidence in the horizontal plane. To minimize the influence of ASE, a preamplifier and a saturable absorber for temporal pulse cleaning was added to the laser system to provide a main pulse to ASE intensity contrast ratio greater than  $10^{10}$  at 1 ns and  $10^9$  at 50 ps before the main pulse. These exceptional ASE conditions allow experiments using an artificial prepulse with intensity below  $10^{11}$  W/cm<sup>2</sup>.

The shock driving steering beam is produced using a frequency doubled (yttrium aluminum garnet) Nd:YAG laser.

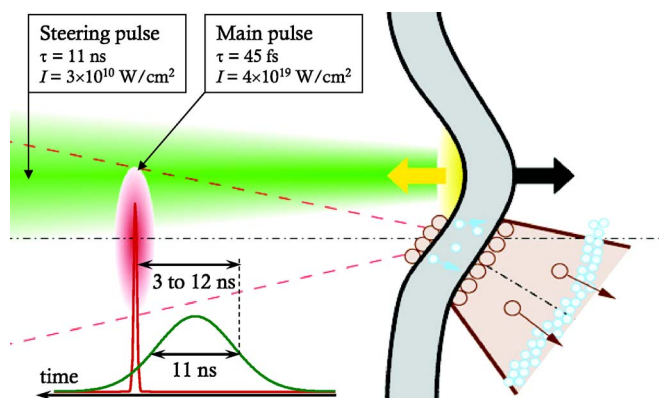


FIG. 1. (Color online) Schematic illustration of the described method for active manipulation of laser accelerated ion beams. Prior to the main pulse interaction, a low intensity pulse ionizes and ablates the front surface of the thin foil target. The induced ablation pressure shocks and locally deforms the foil, shifting the emission direction of the proton beam generated by the high intensity laser pulse.

<sup>a)</sup>Electronic mail: olle.lundh@fysik.lth.se.

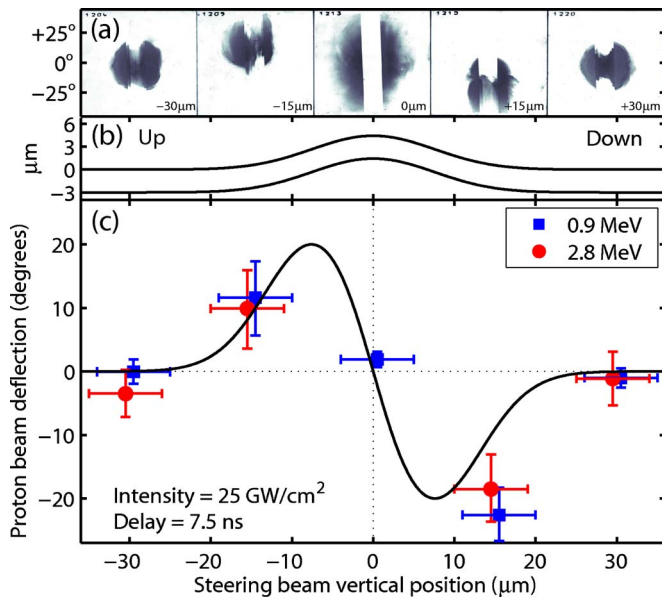


FIG. 2. (Color online) Proton beam deflection as function of the vertical position of the horizontal line focus relative to the high-intensity focal spot. Error bars indicate the relative beam positioning accuracy and the total spread of the deflection data over three consecutive shots. Representative data in (a) illustrates the quality of the deflected proton beams. The calculated shape of the foil when the main pulse arrives on target is shown in (b). The normal direction to this curve, the solid line in (c), fits the data very well.

An 11 ns (FWHM) laser pulse is delivered on the target with an energy up to 50 mJ at 532 nm. To control the arrival time of the steering pulse, the  $Q$  switch in the Nd:YAG oscillator is electronically synchronized to the main laser pulse with a pulse-to-pulse jitter less than 200 ps. The relative delay between the main pulse and the half maximum of the rising edge of the steering pulse is varied between 3 and 12 ns. The steering beam is focused by a 200 mm focal length doublet lens, which has been rotated around the vertical axis in order to produce a horizontal line focus, 14  $\mu\text{m}$  wide and 230  $\mu\text{m}$  long. In this simplified geometry, proton deflection is expected only in the vertical plane.

The spatial distribution of the proton beam is diagnosed using CR39 plastic track detectors, covered by stripes of aluminum stopping filters in order to facilitate simultaneous recording of the spatial distribution above several threshold energies, up to 2.8 MeV.<sup>12</sup>

The steering pulse arrives on the target prior to the main pulse and creates a plasma at the front surface. As the hot plasma is ejected into the vacuum, the induced ablation pressure locally shocks and deforms the target. The magnitude of the deformation depends on the driving laser intensity and on the time available for the target expansion following shock breakout. The emission direction of protons, accelerated from the deformed rear surface by the high-intensity laser pulse, depends on the local target normal direction.<sup>9</sup> To demonstrate active control of the proton emission direction, we systematically vary the intensity, delay, and position of the steering pulse.

Keeping all other parameters constant, we first scan the vertical position of the horizontal line focus relative to the high-intensity focal spot. As shown in Fig. 2, we see no effect when the distance between the main pulse and the steering pulse is 30  $\mu\text{m}$ . This means that the width of the emitting region and the width of the local deformation do not

overlap. When the steering pulse is positioned at  $\pm 15 \mu\text{m}$ , the proton beam is significantly deflected. As expected, the protons are steered upward when the steering pulse is below the main pulse and vice versa. Note that protons of different energies are steered by approximately the same amount. This full beam steering is fundamentally different from the energy dependent beam deflection obtained previously using the intrinsic ASE pedestal<sup>12,13</sup> and indicates that the entire proton source fits on the slope of the deformation. We also note that the number of protons in the deflected proton beams remain similar to the undeflected beams. When the two pulses overlap on the target, the divergence of the low energy part of the proton beam is significantly increased in the vertical direction. We interpret this to be due to the cylindrically convex shape of the emitting rear surface.<sup>13</sup> The absence of higher proton energies indicates that under these conditions, the area close to the peak of the deformation is not suitable for efficient acceleration. A reasonable explanation is the long preplasma scale length resulting from the ablation of the target front. This could increase the divergence of the electron beam driven into the target by the high intensity laser pulse but also reduce the front side reflection of refluxing electrons. Both effects reduce the electron density in the sheath at the rear surface and, thereby, also the magnitude of the accelerating field.

To model the proton emission direction we employ the quasi-two-dimensional scheme presented in Ref. 13. The magnitude of the deformation depends on the time available for the laser-driven shock to transit the target and for expansion following shock breakout. The shock velocity,  $u_s = c_0/2(\sqrt{1+\eta}+1)$ , and the expansion velocity,  $u_e = c_0/\alpha(\sqrt{1+\eta}-1)$ , are derived from the equation of state of the target material. Here,  $\eta = (4\alpha/\rho_0 c_0^2)P$  depends linearly on the laser induced ablation pressure  $P$ ,  $\rho_0$  is the density,  $c_0$  is the sound speed, and  $\alpha$  is a dimensionless parameter of the order of unity. Neglecting transverse shock spreading and using a rectangular approximation of the laser pulse shape, the shape of the rear surface is  $z(x,t) = \max(0, \{t - [L/u_s(x)]\}u_e(x))$ , where  $t$  is the delay between the two laser pulses,  $x$  is the vertical position, and  $L$  is the target thickness. The induced pressure distribution (in pascal) is assumed to follow the intensity distribution (in  $\text{W}/\text{m}^2$ ) as  $P(x) = 1.3I(x)^{2/3}$ , according to the scaling given by Lindl.<sup>15</sup>

Using tabulated data for aluminum ( $\rho_0 = 2.7 \text{ g}/\text{cm}^3$ ,  $c_0 = 5240 \text{ m}/\text{s}$ , and  $\alpha = 1.40$ ) and a Gaussian intensity distribution with a 14  $\mu\text{m}$  full width at half maximum, the shape of the target foil at the time of the main pulse arrival on target is calculated [see Fig. 2(b)]. The direction of the local target normal, shown by the solid line in Fig. 2(c), fits the measured data very well. The model indirectly gives an upper limit to the proton source size. The region in which the proton beam is steered has a width of 40  $\mu\text{m}$  so the proton emitting area must be smaller than 20  $\mu\text{m}$  for protons above the detection threshold (0.9 MeV). This is small compared to previous studies.<sup>2</sup> The reasons are the thinner targets and shorter pulses used in this experiment. We can estimate the expected source size by simply assuming that electrons, injected at angle  $\theta$ , recirculate inside the target during the laser pulse and are ballistically reflected at the surfaces. After the laser pulse has passed, we estimate the sheath radius at the rear as  $R = r + (c\tau + L)\tan\theta$ . Here,  $r$  is the focal spot radius and  $\theta$  is the half opening angle of the injected electron dis-

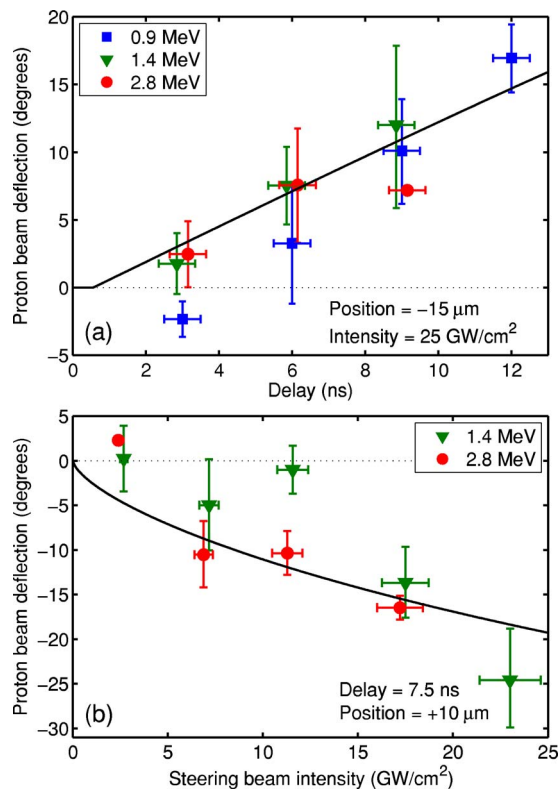


FIG. 3. (Color online) Deflection of protons of different energies as function of (a) delay and (b) intensity of the steering pulse. When the line focus is below the main pulse, protons are steered upward and vice versa. Vertical error bars show the total spread of the deflection data over three consecutive shots. The summed uncertainty due to drift and pulse-to-pulse fluctuations are shown by the horizontal error bars.

tribution. For a full opening angle of  $30^\circ$  and our experimental parameters, the predicted sheath diameter is  $14\text{ }\mu\text{m}$ , which agrees well with our experimental observations.

We now keep the steering beam fixed at a  $15\text{ }\mu\text{m}$  offset below the main focal spot and vary the relative delay between the two pulses [see Fig. 3(a)]. As expected, the proton beam is deflected upward with a magnitude that increases with increasing delay. As in Fig. 2, the magnitude of the deflection does not vary significantly for protons of different energies and the analytical model fits the data very well. Note that prior to shock breakout, we expect no proton beam deflection since the rear surface is unperturbed. Finally, we vary the intensity of the steering beam [see Fig. 3(b)]. Note that, even though the model qualitatively fits the data, target ionization is not included and at laser intensities close to or below the ionization threshold, the induced ablation pressure cannot be accurately estimated.

In conclusion, we have demonstrated a method for optical control of the spatial distribution of laser-accelerated proton beams. In this letter, we concentrated on the first-order application of the method, beam steering, but by using tailored intensity distributions, other aspects of the spatial dis-

tribution should be possible to control. We expect that a ring shaped beam can control the ion beam divergence and that the dynamic change of the target curvature can bring the proton beam to focus at an adjustable distance from the foil. Such control is very interesting for many applications such as studies of isochoric heating of dense plasmas and for the fast ignition approach to inertial confinement fusion. In addition, by controlling the divergence directly at the source, a higher charge could be delivered into the limited acceptance angle of the injection optics in a large accelerator.

The authors acknowledge discussions with D. Neely and financial support from the Swedish Research Council and the Knut and Alice Wallenberg Foundation. C.H. was supported by the Marie Curie EST MAXLAS program. P.McK. and D.C. acknowledge the support from the COST P-14 program.

- <sup>1</sup>L. Robson, P. Simpson, R. Clarke, K. W. D. Ledingham, F. Lindau, O. Lundh, T. McCanny, P. Mora, D. Neely, C.-G. Wahlstrom, M. Zepf, and P. McKenna, *Nat. Phys.* **3**, 58 (2007).
- <sup>2</sup>T. E. Cowan, J. Fuchs, H. Ruhl, A. Kemp, P. Audebert, M. Roth, R. Stephens, I. Barton, A. Blazevic, E. Brambrink, J. Cobble, J. Fernandez, J.-C. Gauthier, M. Geissel, M. Hegelich, J. Kaae, S. Karsch, G. P. LeSage, S. Letzring, M. Manclossi, S. Meyroneinc, A. Newkirk, H. Pepin, and N. Renard-LeGalloudec, *Phys. Rev. Lett.* **92**, 204801 (2004).
- <sup>3</sup>M. Borghesi, A. J. Mackinnon, D. H. Campbell, D. G. Hicks, S. Kar, P. K. Patel, D. Price, L. Romagnani, A. Schiavi, and O. Willi, *Phys. Rev. Lett.* **92**, 055003 (2004).
- <sup>4</sup>S. V. Bulanov and V. S. Khoroshkov, *Plasma Phys. Rep.* **28**, 453 (2002).
- <sup>5</sup>K. W. D. Ledingham, P. McKenna, T. McCanny, S. Shimizu, J. M. Yang, L. Robson, J. Zweit, J. M. Gillies, J. Bailey, G. N. Chimon, R. J. Clarke, D. Neely, P. A. Norreys, J. L. Collier, R. P. Singhal, M. S. Wei, S. P. D. Mangles, P. Nilson, K. Krushelnick, and M. Zepf, *J. Phys. D* **37**, 2341 (2004).
- <sup>6</sup>K. Krushelnick, E. L. Clark, R. Allott, F. N. Beg, C. N. Danson, A. Machacek, V. Malka, Z. Najmudin, D. Neely, P. A. Norreys, M. R. Salvati, M. I. K. Santala, M. Tatarakis, I. Watts, M. Zepf, and A. E. Dangor, *IEEE Trans. Plasma Sci.* **28**, 1184 (2000).
- <sup>7</sup>M. Roth, T. E. Cowan, M. H. Key, S. P. Hatchett, C. Brown, W. Fountain, J. Johnson, D. M. Pennington, R. A. Snavely, S. C. Wilks, K. Yasuike, H. Ruhl, F. Pegoraro, S. V. Bulanov, E. M. Campbell, M. D. Perry, and H. Powell, *Phys. Rev. Lett.* **86**, 436 (2001).
- <sup>8</sup>M. Borghesi, J. Fuchs, S. V. Bulanov, A. J. MacKinnon, P. K. Patel, and M. Roth, *Fusion Sci. Technol.* **49**, 412 (2006).
- <sup>9</sup>S. C. Wilks, A. B. Langdon, T. E. Cowan, M. Roth, M. Singh, S. Hatchett, M. H. Key, D. Pennington, A. MacKinnon, and R. A. Snavely, *Phys. Plasmas* **8**, 542 (2001).
- <sup>10</sup>P. K. Patel, A. J. Mackinnon, M. H. Key, T. E. Cowan, M. E. Ford, M. Allen, D. F. Price, H. Ruhl, P. T. Springer, and R. Stephens, *Phys. Rev. Lett.* **91**, 125004 (2003).
- <sup>11</sup>F. N. Beg, M. S. Wei, A. E. Dangor, A. Gopal, M. Tatarakis, K. Krushelnick, P. Gibbon, E. L. Clark, R. G. Evans, K. L. Lancaster, P. A. Norreys, K. W. D. Ledingham, P. McKenna, and M. Zepf, *Appl. Phys. Lett.* **84**, 2766 (2004).
- <sup>12</sup>F. Lindau, O. Lundh, A. Persson, P. McKenna, K. Osvay, D. Batani, and C.-G. Wahlstrom, *Phys. Rev. Lett.* **95**, 175002 (2005).
- <sup>13</sup>O. Lundh, F. Lindau, A. Persson, C.-G. Wahlstrom, P. McKenna, and D. Batani, *Phys. Rev. E* **76**, 026404 (2007).
- <sup>14</sup>D. Neely, P. Foster, A. Robinson, F. Lindau, O. Lundh, A. Persson, C.-G. Wahlstrom, and P. McKenna, *Appl. Phys. Lett.* **89**, 021502 (2006).
- <sup>15</sup>J. Lindl, *Phys. Plasmas* **2**, 3933 (1995).